Journal of Environmental Science and Engineering A 10 (2021) 56-75
doi:10.17265/2162-5298/2021.02.003

Pigment Adsorption Optimization in Various Low Cost Adsorbents

Odysseas Kopsidas
Department of Industrial Management and Technology, University of Piraeus, Piraeus 18534, Greece

Abstract: The applications of adsorption are very important. The following is a list of some of the most common: using the adsorption effect we can achieve a high vacuum in cases of low temperature at which the adsorption of gases from solids is intense. Regarding, the gap we can achieve is in the range of 10-7 mmHg. Another very important application of adsorption is the separation of a mixture of gases from a certain adsorbent, which has a separate adsorption capacity for each gas. In this way it is possible to separate the noble gases, as well as gasoline and hexanes from oil. The experimental diagrams confirm the validity of the Freundlich equation for dilute solutions with low concentrations. At the same time, from the aggregate diagrams of the dilute solutions, listed above, we observe: for graph 1 concerning the adsorbent materials we used we observe that the capacity K_F has a higher value for the ground cork while the lower one for olive ash. Also, for graph 2 regarding the adsorbent materials we used we observe the n of the isothermal Freundlich has a maximum for olive ash while a minimum has for two materials lentil straw and ground cork.

Key words: Adsorption, methylene blue, biomass, adsorbent, fixed bed column studies.

1. Introduction

One of the main applications of adsorption is chromatography. Another application is the purification of water using activated carbon as an adsorbent, as well as its use in anti-asphyxiation masks, to protect against toxic gases [1]. The function of adsorption is widespread in industry. After the adsorption process the adsorbent can be discarded after one use [2]. In practice, however, the economics of the process make it necessary to regenerate the adsorbent with the ultimate goal of reusing it. In industry, activated carbon is typically used as an adsorbent which can be regenerated either chemically or thermally. In chemical regeneration, activated carbon comes into contact with chemicals that decompose or oxidize the adsorbed foreign bodies [3, 4]. Chemical regeneration is only partially effective in restoring the ability to adsorb on activated carbon and is therefore of little use [5].

In chemical regeneration, activated carbon comes in contact with chemicals that decompose or oxidize the adsorbed foreign bodies [6, 7]. The thermal regeneration process of activated carbon has three main steps: the evaporation of water close to 100 °C, baking of activated carbon at temperatures up to 800 °C, its activation between 800 °C and 950 °C. The losses of carbon during the hot regeneration usually range from 5-10% of its amount. Therefore with this method a reduction of the costs of the adsorption process is achieved.

Corresponding author: Odysseas Kopsidas, Ph.D., research field: environmental economics.

2. Methodology

We use as following: H_2O and methylene blue, 0.5 g of sawdust per bottle, 1st bottle: 0 mL H_2O and 500 mL methylene blue, 2nd bottle: 150 mL H_2O and 350 mL methylene blue, 3rd bottle: 250 mL H_2O and 250 mL methylene blue, 4th bottle: 350 mL H_2O and 150 mL methylene blue, 5th bottle: 400 mL H_2O and 100 mL methylene blue, 6th bottle: 450 mL H_2O and 50 mL methylene blue, 7th bottle: 455 mL H_2O and 45 mL methylene blue, 8th bottle: 465 mL H_2O and 35 mL methylene blue , 9th bottle: 475 mL H_2O and 25 mL methylene blue, 10th bottle: 485 mL H_2O and 15

mL methylene blue, 11th bottle: 490 mL H_2O and 10 mL methylene blue, 12th bottle: 495 mL H_2O and 5 mL methylene blue, 500 mL beaker, stirrer, volumetric cylinder, 10 mL pipettes, UV/VIS (Ultraviolet-Visible) spectrophotometer connected to Rinter, 6-position "carousel" and 1 × 1 cm disposable base cupboards for visible light spectrum, nylon filters 0.64 mm, stand with 12 medium-sized test tubes (at least 10 mL), and centrifuge.

Place the predetermined amount of H_2O and methylene blue in the 12 bottles (as shown in the proportions in the materials). After filling 1 test tube, take 10 mL from each bottle, fill and place cuvettes in the "carousel" (the first cuvette is filled with deionized water), for the first 6 bottles dilute 5:100 and fill 3 cuvettes, for the other 6 bottles do not dilute and fill 2 cubes. Measure the ABS (Absorption) in each sample with the UV/VIS spectrophotometer for wavelength λ = 664 nm for methylene blue (see appendix for the other pigments) and save the values on the PC, pour 0.5 gr of sawdust in each bottle, and stir. After 7 days take a sample of 10 mL of each solution with a siphon, store them in test tubes and put them in the centrifuge for 5 minutes to remove sawdust, repeat steps 2 and 3, we save all the results on the PC.

3. Implementation

For dilute solutions the Freundlich adsorption isotherm can be written as [8, 9]:

$$q = K_F \cdot C^{\frac{1}{n}} \tag{1}$$

where q = mg/g of adsorbent, C = mg/L of adsorbent and n, K_F are constant. Eq. (1) describes the equilibrium conditions.

$$\log q = \log K_F + \frac{1}{n} \log C_e \tag{2}$$

Langmuir (1916) adsorption isotherm can be written as:

$$\frac{1}{q} = \left(\frac{1}{q_m}\right) + \left(\frac{1}{K_L \cdot q_m}\right) \cdot \left(\frac{1}{C_e}\right) \tag{3}$$

In Fig. 1, it is shown the determination of the optimal pigment concentration in the treated dye waste.

Finally, we calculate the standard deviation error where n is the measurement we made (n = 10) and p is the parameters (p = 3, i.e. a, b, C_∞). For the various values, we assume we will have the corresponding deviations s. For the smallest value of s (the one that is closer to 0) we will have both its optimal value, and k. For these values, we calculate it and make its graph as a function of time.

Fixed bed column studies: The experiments on the adsorption columns were performed on a column 15 × 2.5 cm in diameter. The height of the column was 15 cm. The amount of adsorbent was about 20 g. The flow was adjusted from 10, 20 and 40 mL·min^{-1} using pump, LaPrep P110-VWR-VWR International. The experiments on the adsorption columns were performed at a constant ambient temperature, i.e. 23-25 °C. The initial concentration of the solution for MB (Methylene Blue) was 14 and 190 mg·L^{-1} and the pH was 8, respectively. The initial concentration of the solution for Cr (VI) was about 75 mg·L^{-1} and the pH of the solution was 2. To determine the concentration of Cr (VI) and MB in the effluent, the effluent samples were taken per 100 mL. The main mathematical models the author used to interpret the results from the experiments in the columns were mainly the Bohart-Adams model which is the most common according to the literature, the Clark model and the Modified Dose Response model which are relatively recent and it was observed that the results of the experiments in the columns for hexavalent chromium adapt very well to this model [10, 11]. All the models the author mentioned above are presented in their non-linear format for the results of the experiments in columns. The author quoted in detail figures for both the dye methylene blue and the hexavalent chromium for the raw materials pine sawdust and spruce sawdust as well as for the pre-treated materials respectively.

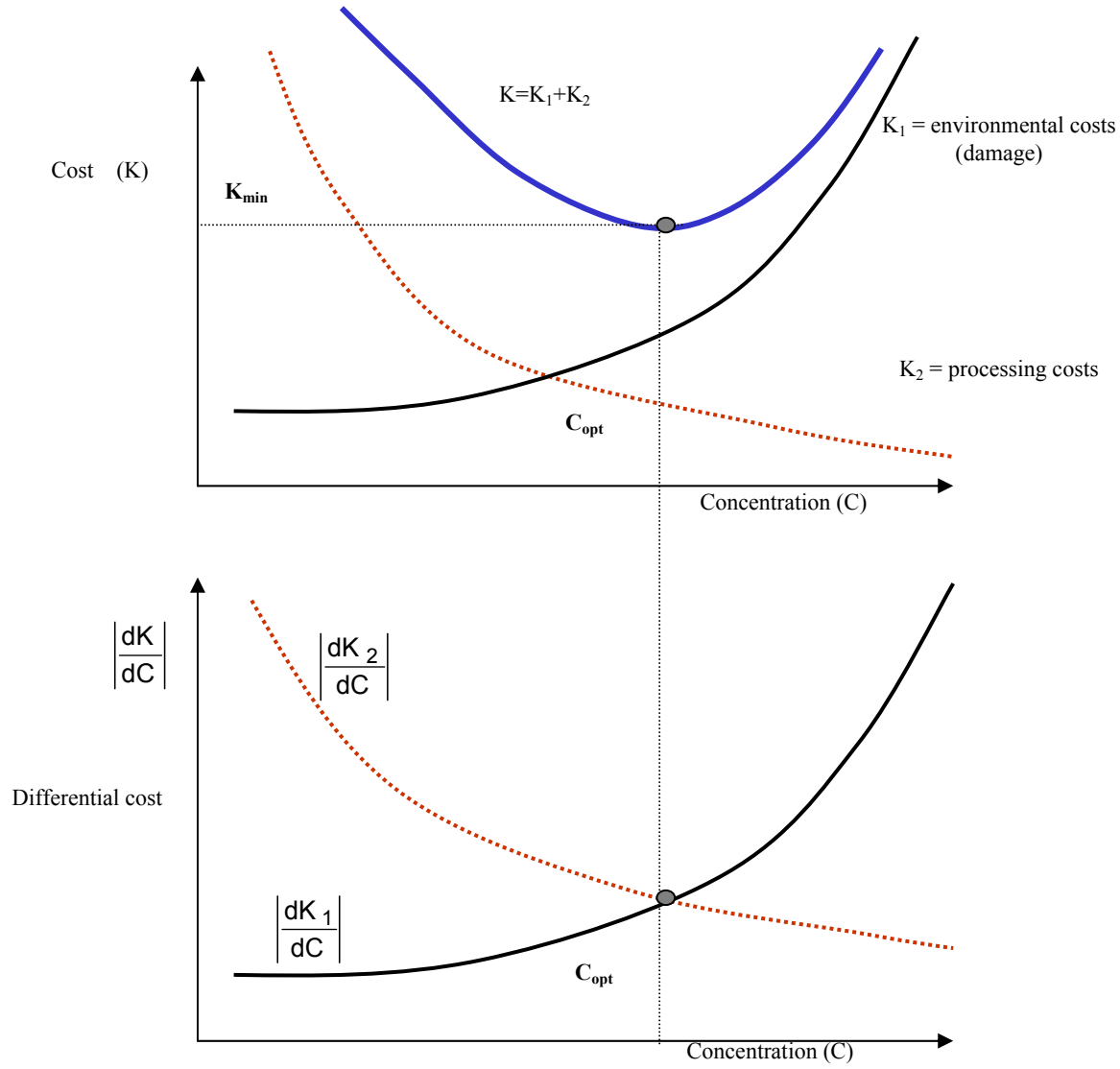

The optimum is at the intersection of the differential cost curves.

$$\frac{dK_t}{dC} = \frac{d(K_1 + K_2)}{dC} = 0 \Rightarrow \frac{dK_1}{dC} + \frac{dK_2}{dC} = 0 \Rightarrow \frac{dK_1}{dC} - \left(-\frac{dK_2}{dC}\right) = 0$$

$$\frac{dK_2}{dC} < 0 \quad \left|\frac{dK_1}{dC}\right| - \left|\frac{dK_2}{dC}\right| = 0 \Rightarrow \left|\frac{dK_1}{dC}\right| = \left|\frac{dK_2}{dC}\right|$$

Fig. 1 Determination of the optimal pigment concentration in the treated dye waste.

Table 1 Experiment 1: raw spruce sawdust.

t (h)	C_1	C_2	C_3	C_4	C_5	C_6	C_7	C_8	C_9	C_{10}	C_{11}	C_{12}
0.00	133.69	113.94	84.24	42.98	34.47	17.30	12.89	9.98	6.74	4.32	2.99	2.02
168.00	111.31	83.08	54.80	25.46	14.54	4.28	3.36	2.88	1.70	0.81	0.40	0.28
C_e	111.31	83.08	54.80	25.46	14.54	4.28	3.36	2.88	1.70	0.81	0.40	0.28
q	22.39	30.87	29.45	17.52	19.93	13.02	9.52	7.09	5.04	3.51	2.58	1.74
logC_e	2.0465	1.9194	1.7387	1.406	1.162	0.632	0.527	0.46	0.22	-0.09	-0.39	-0.56
log$q$	1.3499	1.4894	1.4690	1.244	1.3	1.115	0.979	0.85	0.70	0.546	0.412	0.24

logK_F	0.628757
$1/n$	0.457399
K_F	4.253602
n	2.186274
R	0.963642
R^2	0.928606

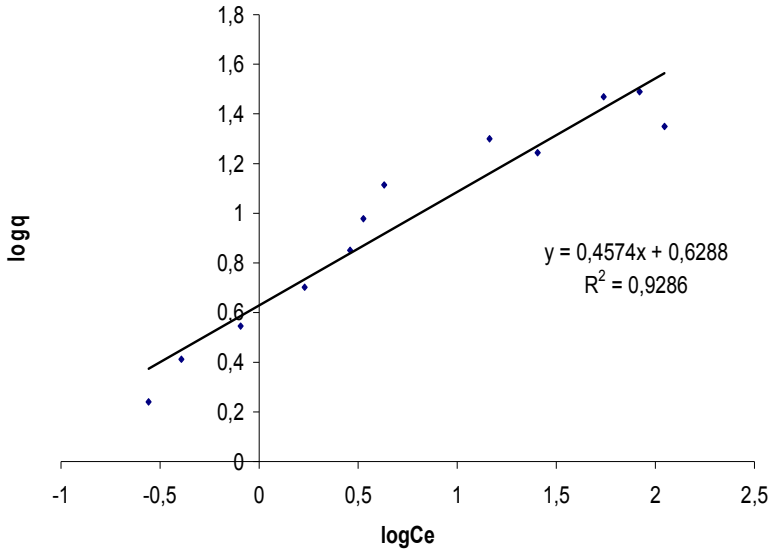

Fig. 2 Experiment 1: raw spruce sawdust: 0.5 gr.

Table 2 Experiment 2: olive ash.

t (h)	C_1	C_2	C_3	C_4	C_5	C_6	C_7	C_8	C_9	C_{10}	C_{11}	C_{12}
0.00	140.10	97,41	78.13	49.14	33.61	18.74	12.55	9.69	7.08	4.26	3.16	1.46
168.00	124.95	94.44	73.07	44.51	26.30	13.07	9.51	6.77	5.44	3.50	2.30	1.02
C_e	124.95	94.44	73.07	44.51	26.30	13.07	9.51	6.77	5.44	3.50	2.30	1.02
q	15.14	2.97	5.07	4.63	7.31	5.67	3.04	2.93	1.63	0.75	0.86	0.44
logC_e	2.0967	1.9751	1.8637	1.648	1.42	1.116	0.978	0.83	0.73	0.544	0.361	0.009
log$q$	1.1802	0.4723	0.7046	0.666	0.864	0.754	0.482	0.46	0.21	-0.12	-0.07	-0.36

logK_F	-0.21059
1/n	0.572908
K_F	0.615757
n	1.745481
R	0.860552
R^2	0.74055

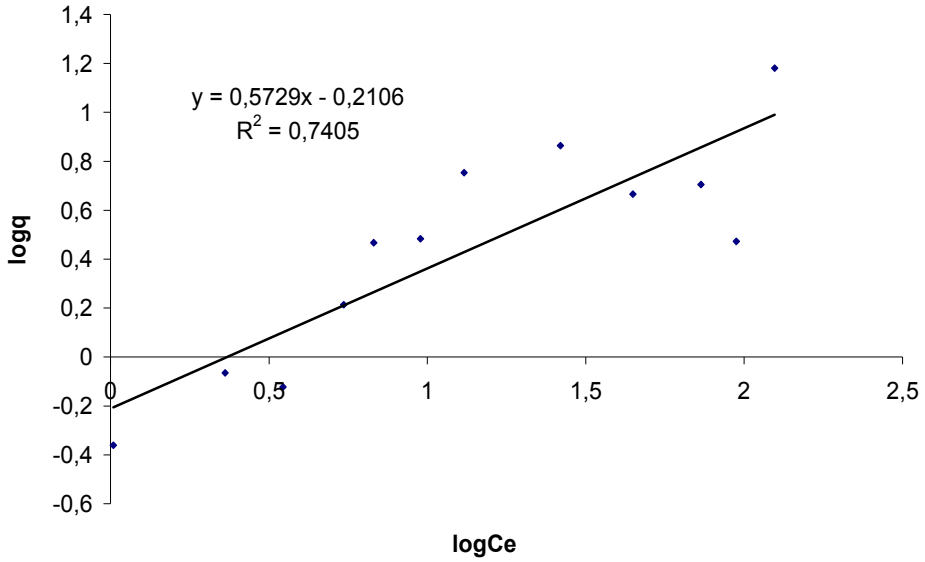

Fig. 3 Experiment 2: olive ash.

Table 3 Experiment 3: seaweed.

t (h)	C_1	C_2	C_3	C_4	C_5	C_6	C_7	C_8	C_9	C_{10}	C_{11}	C_{12}
0.00	141.30	108.78	79.73	48.05	35.46	16.00	12.03	9.42	6.79	4.45	3.04	1.60
168.00	46.50	34.15	21.09	9.31	6.77	2.79	2.11	1.49	0.89	0.59	0.41	0.39
C_e	46.50	34.15	21.09	9.31	6.77	2.79	2.11	1.49	0.89	0.59	0.41	0.39
q	94.80	74.63	58.64	38.74	28.69	13.20	9.92	7.94	5.91	3.87	2.64	1.20
logC_e	1.6674	1.5333	1.3241	0.969	0.831	0.446	0.324	0.172	-0.05	-0.23	-0.39	-0.4
log$q$	1.9768	1.8729	1.7682	1.588	1.458	1.121	0.996	0.9	0.771	0.587	0.42	0.08

logK_F	0.710719
$1/n$	0.809791
K_F	5.137109
n	1.234886
R	0.982619
R^2	0.96554

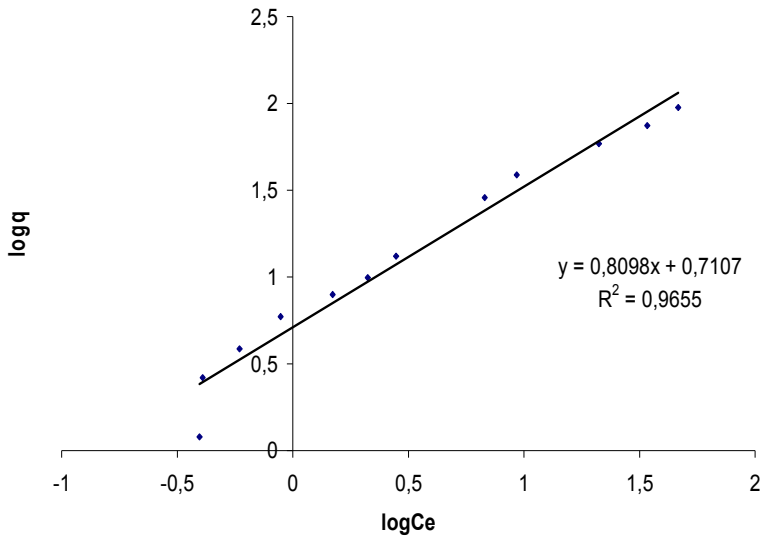

Fig. 4 Experiment 3: seaweed.

Table 4 Experiment 4: peach seeds.

t (h)	C_1	C_2	C_3	C_4	C_5	C_6	C_7	C_8	C_9	C_{10}	C_{11}	C_{12}
0.00	139.04	108.98	82.06	52.76	37.53	31.58	12.02	9.32	6.59	4.53	2.85	1.64
168.00	123.81	102.35	69.46	38.58	11.43	10.12	9.49	5.80	5.18	3.71	1.88	1.06
C_e	123.81	102.35	69.46	38.58	11.43	10.12	9.49	5.80	5.18	3.71	1.88	1.06
q	15.23	6.62	12.60	14.18	26.09	21.46	2.53	3.52	1.41	0.81	0.97	0.58
logC_e	2.0927	2.0100	1.8417	1.586	1.058	1.005	0.977	0.763	0.715	0.57	0.27	0.02
log$q$	1.1826	0.8210	1.1003	1.152	1.417	1.332	0.402	0.546	0.15	-0.09	-0.01	-0.23

logK_F	-0.06556
$1/n$	0.662242
K_F	0.859879
n	1.510021
R	0.74926
R^2	0.56139

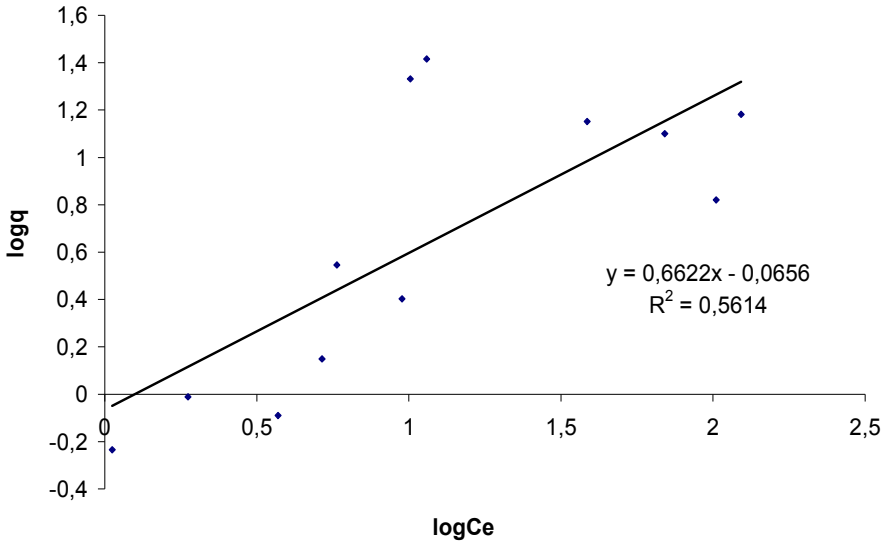

Fig. 5 Experiment 4: peach seeds.

Table 5 Experiment 5: raw lentils.

t (h)	C_1	C_2	C_3	C_4	C_5	C_6	C_7	C_8	C_9	C_{10}	C_{11}	C_{12}
0.00	144.05	109.44	84.03	53.55	37.02	21.71	12.80	10.20	7.63	4.69	3.39	1.80
168.00	86.42	65.80	25.38	12.06	8.59	6.88	4.69	4.54	4.08	2.64	1.77	1.13
C_e	86.42	65.80	25.38	12.06	8.59	6.88	4.69	4.54	4.08	2.64	1.77	1.13
q	57.63	43.64	58.64	41.50	28.43	14.83	8.11	5.65	3.55	2.04	1.62	0.68
$\log C_e$	1.9366	1.8182	1.4045	1.081	0.934	0.838	0.671	0.657	0.61	0.422	0.24	0.05
$\log_q$	1.7606	1.6399	1.7682	1.618	1.454	1.171	0.909	0.752	0.551	0.311	0.20	-0.17

$\log K_F$	0.072773
$1/n$	1.040063
K_F	1.182425
n	0.96148
R	0.909878
R^2	0.827878

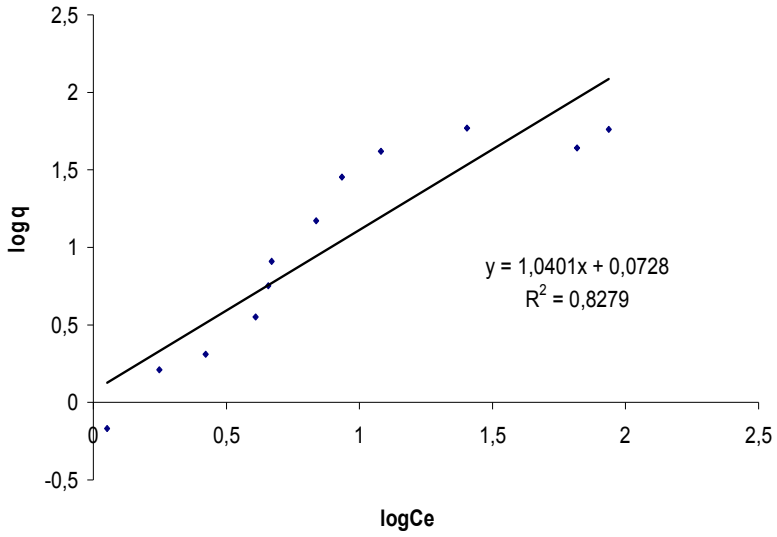

Fig. 6 Experiment 5: raw lentils.

Table 6 Experiment 6: lentil ground with spherical apple for 15 min.

t (h)	C_1	C_2	C_3	C_4	C_5	C_6	C_7	C_8	C_9	C_{10}	C_{11}	C_{12}
0.00	137.68	109.52	81.88	53.58	36.56	14.59	12.79	9.89	6.98	4.39	3.25	1.58
168.00	22.41	6.72	7.18	2.96	2.59	2.84	3.63	3.00	3.63	2.08	1.38	0.70
C_e	22.41	6.72	7.18	2.96	2.59	2.84	3.63	3.00	3.63	2.08	1.38	0.70
q	115.27	102.79	74.71	50.62	33.98	11.75	9.17	6.89	3.35	2.31	1.87	0.88
logC_e	1.3504	0.8276	0.8558	0.472	0.413	0.453	0.559	0.477	0.56	0.317	0.13	-0.16
log$q$	2.0617	2.0119	1.8733	1.704	1.531	1.07	0.962	0.838	0.525	0.364	0.27	-0.06

logK_F	0.262804
$1/n$	1.595953
K_F	1.831487
n	0.626585
R	0.822097
R^2	0.675844

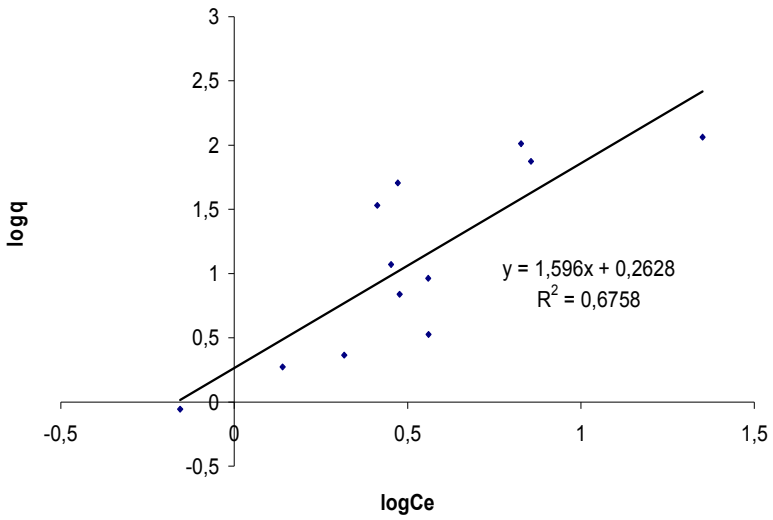

Fig. 7 Experiment 6: lentil ground with spherical apple for 15 min.

Table 7 Experiment 7: ground cork.

t (h)	C_1	C_2	C_3	C_4	C_5	C_6	C_7	C_8	C_9	C_{10}	C_{11}	C_{12}
0.00	137.21	109.42	86.93	53.13	36.24	18.03	12.97	10.09	7.00	4.30	3.05	1.63
168.00	121.32	81.05	48.55	30.43	18.36	5.92	1.59	1.11	1.24	0.75	0.58	0.41
C_e	121.32	81.05	48.55	30.43	18.36	5.92	1.59	1.11	1.24	0.75	0.58	0.41
q	15.90	28.36	38.37	22.70	17.88	12.11	11.38	8.98	5.76	3.54	2.47	1.22
logC_e	2.0839	1.9087	1.6862	1.483	1.264	0.772	0.201	0.046	0.094	-0.12	-0.23	-0.39
log$q$	1.2012	1.4527	1.5840	1.356	1.252	1.083	1.056	0.953	0.76	0.549	0.39	0.08

logK_F	0.659616
$1/n$	0.433181
K_F	4.566842
n	2.308503
R	0.868553
R^2	0.754384

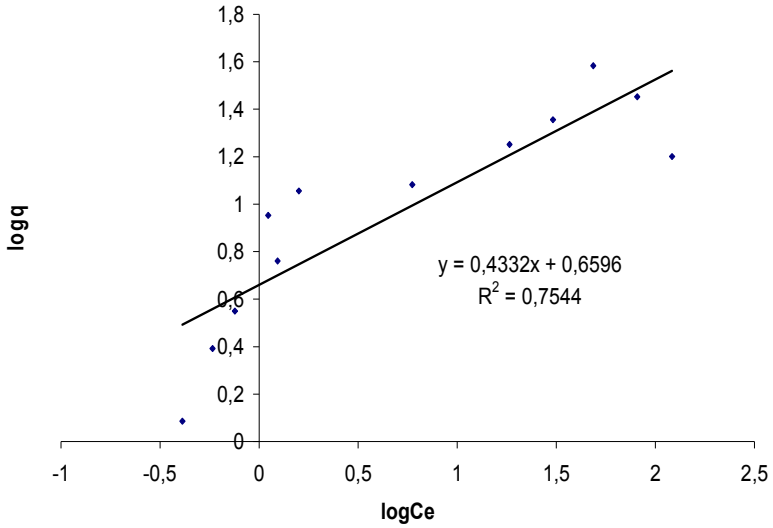

Fig. 8 Experiment 7: ground cork.

Table 8 Experiment 8: chickpea straw.

t (h)	C_1	C_2	C_3	C_4	C_5	C_6	C_7	C_8	C_9	C_{10}	C_{11}	C_{12}
0.00	146.92	111.48	81.25	51.22	34.60	17.30	14.05	9.77	6.90	4.60	3.03	1.86
168.00	60.69	21.94	33.34	8.43	7.56	6.93	3.69	3.95	2.70	1.92	1.16	0.69
C_e	60.69	21.94	33.34	8.43	7.56	6.93	3.69	3.95	2.70	1.92	1.16	0.69
q	86.23	89.54	47.91	42.79	27.04	10.37	10.37	5.82	4.20	2.67	1.88	1.17
logC_e	1.7831	1.3413	1.5230	0.926	0.879	0.841	0.567	0.596	0.431	0.284	0.06	-0.16
log$_q$	1.9356	1.9520	1.6804	1.631	1.432	1.016	1.016	0.765	0.623	0.427	0.27	0.06

logK_F	0.263581
1/n	1.064261
K_F	1.834769
n	0.93962
R	0.950407
R^2	0.903273

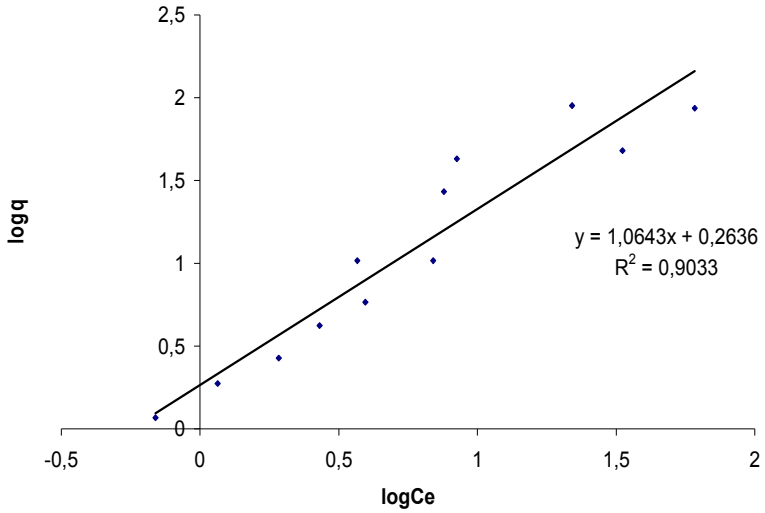

Fig. 9 Experiment 8: chickpea straw.

Table 9 Aggregated data.

Materials	Exp. 1	Exp. 2	Exp. 3	Exp.4	Exp.5	Exp.6	Exp.7	Exp.8
logK_F	0.6043	0.7271	0.7404	-0.2687	0.2034	-0.2415	0.1063	-0.4265
1/n	0.6074	1.0426	1.6007	0.7149	1.0959	1.5078	1.1947	0.9168
K_F	4.0211	5.3343	5.5011	0.5387	1.5973	0.5734	1.2773	0.3746
n	1.6463	0.9592	0.6247	1.3988	0.9125	0.6632	0.8370	1.0907
R	0.9888	0.9219	0.9707	0.8323	0.9506	0.9678	0.8964	0.9462
R^2	0.9776	0.8500	0.9422	0.6927	0.9037	0.9367	0.8035	0.8953

Table 10 Summary table of parameters of Bohart-Adams and Clark models of raw and self-hydrolyzed pine sawdust for MB removal (self-hydrolysis conditions: 240 °C, isothermal reaction time 40 min).

	C_i (mg·L^{-1})	Q (mg·g^{-1})	n	N (mg·L^{-1})	K (L·mg^{-1}·min^{-1})	*SEE*
Raw spruce sawdust						
Bohart-Adams	192	46		8.046	0.00050	7.58
Bohart-Adams	14	10		8.722	0.00134	0.194
Clark	192	46	2.500	8.723	0.00058	8.75
Clark	14	10	2.500	8.781	0.00159	0.201
Self-hydrolyzed at 240 °C for 40 min spruce sawdust						
Bohart-Adams	192	46		14.157	0.00034	7.13
Bohart-Adams	14	10		14.313	0.00072	0.179
Clark	192	46	2.582	15.132	0.00042	8.47
Clark	14	10	2.582	14.429	0.00087	0.217

In Table 10, we observe the parameters of the Bohart-Adams and Clark models for nonlinear analysis, for the removal of Methylene Blue dye using crude and self-hydrolyzed pine sawdust at 240 °C, geothermal reaction time 40 minutes. In detail we see that the experiments have been done in different concentrations and flows. Theoretical calculations according to the Bohart-Adams model sufficiently verify the experimental data according to Figs. 11-12.

It is obvious from the Table 11 but also from Figs. 10 -11 that the pretreatment of our material has improved its adsorption capacity. This can be observed from both mathematical models that we analyze if we compare the results and the raw material. For example, n equals 8,046 for raw pine sawdust while for self-hydrolyzed at 240 ^{o}C for 40 minutes under the same conditions n equals 14,157.

In addition, the Standard Error of the Estimate (*SEE)* values of the standard estimation error are given in table. According to them, the adaptability of the Bohart-Adams model to the experimental data was found to be better than that of the Clark model for the methylene blue dye. It should be noted that parameter n in the Clark model is given by the previously presented Freundlich isotherm.

In Tables 11-12, we see the parameters of the Bohart-Adams and Modified Dose-Response models of crude and self-hydrolyzed pine sawdust for Cr (VI) removal. The pretreatment conditions of self-hydrolyzed pine sawdust are 160, 200 and 240 °C and the isothermal reaction times 0 and 50 minutes. The volume of the solution V (L) of the hexavalent chromium is equal to $V = Q \cdot t$ where Q is the flow rate of the hexavalent solution chromium and is equal to 20 mL·min^{-1}. The mass of the material was 20 g and the concentration of hexavalent chromium was 75 mg·L^{-1}. Observing Table 11, we see that the n for the raw pine sawdust is equal to 390 while for our most extreme pre-treatment that is self-hydrolysis at 240 °C for 50 minutes is 4,746, which is the maximum. Respectively according to Table 11, the q_o for the raw material is 1.30 mg·g^{-1} while for the self-hydrolyzed at 240 °C for 50 minutes it is equal to 23.71 mg·g^{-1}.

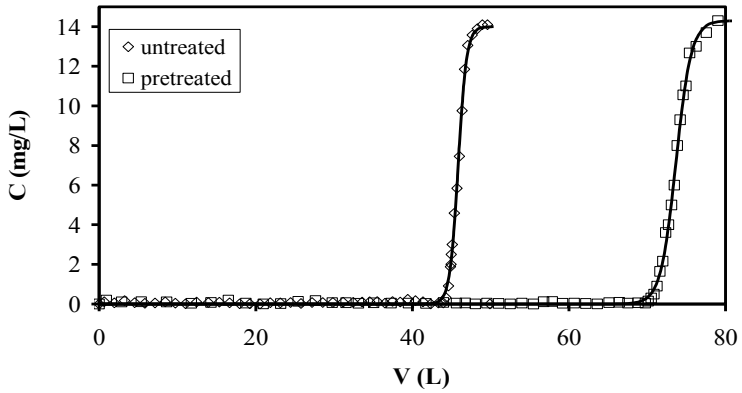

Fig. 10 Curves of methylene blue for C (mg·L^{-1}) as a function of V (mL) according to the Bohart-Adams model for raw and self-hydrolyzed at 240 °C for 40 minutes pine sawdust (adsorption conditions: x = 15 cm, E = 4.9 cm^2, Q = 10 mL·min^{-1}, m = 22 g, C_i = 14 mg·L^{-1}, pH = 8).

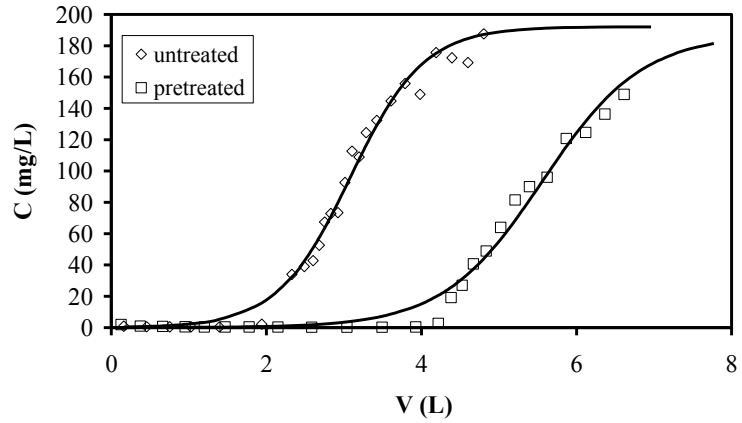

Fig. 11 Curves of methylene blue for C (mg·L^{-1}) as a function of V (mL) according to the Bohart-Adams model for raw and self-hydrolyzed at 240 °C for 40 minutes pine sawdust (adsorption conditions: x = 15 cm, E = 4.9 cm^2, Q = 46 mL·min^{-1}, m = 22 g, C_i = 192 mg·L^{-1}, pH = 8).

The Modified Dose-Response model [12-14] shows that the self-hydrolyzed material in extreme conditions (240 °C for 50 minutes) increases its adsorption capacity by 37 times compared to the raw material. In Fig. 12, we see the theoretical curves for the Modified Dose-Response model for all three autodrolysis temperatures but only for the extreme isothermal reaction time, i.e. 50 minutes. The adaptability of the Modified Dose-Response model to the experimental data was found to be better than that of the Bohart-Adams model for hexavalent chromium.

In Table 12, we observe the parameters of the Bohart-Adams and Modified Dose-Response models of crude and pre-treated spruce sawdust for Cr (VI) removal. The pretreatment conditions of spruce sawdust are with 50% diethylene glycol, 50% H_2O, 0.045 N H_2SO_4, at 160, 180, 200 and 220 °C and an isothermal reaction time of 50 minutes. The experiments were performed at a flow rate of 20 mL·min^{-1}, the mass of the material was 20 g and the concentration of hexavalent chromium was 75 mg·L^{-1}.

Observing Table 13, we see that the n for the raw spruce sawdust is equal to 101 while for the raw material with 50% diethylene glycol, 50% H_2O, 0.045 N H_2SO_4, at 180 °C and an isothermal reaction time of 50 minutes is 2,092. maximum, while for our extreme pretreatment, i.e. 50% diethylene glycol, 50% H_2O, 0.045 N H_2SO_4, at 220 °C and an isothermal reaction

Table 11 Summary table of Bohart-Adams model parameters of crude and self-hydrolyzed pine sawdust for Cr (VI) removal (pre-treatment conditions: 160, 200 and 240 °C, isothermal reaction times 0 and 50 minutes).

Bohart-Adams model				
	n (mg·L^{-1})	K	q_o (mg·g^{-1})	*SEE*
160 °C				
-	390	0.00036	1.30	9.05
0	-320	0.00013	-1.24	5.94
50	715	0.00042	2.77	6.67
200 °C				
0	1,594	0.00015	5.86	7.46
50	2,371	0.00020	7.93	5.91
240 °C				
0	4,067	0.00028	14.96	1.98
50	4,746	0.00024	19.40	2.23

Table 12 Summary table of parameters of the Modified Dose-Response model of crude and self-hydrolyzed pine sawdust for Cr (VI) removal (pre-treatment conditions: 160, 200 and 240 °C, isothermal reaction times 0 and 50 minutes).

Modified Dose-Response model			
	a_{mdr}	q_o (mg·g^{-1})	*SEE*
160 °C			
-	0.76	0.64	2.11
0	0.55	1.00	2.89
50	0.92	2.18	4.46
200 °C			
0	0.71	4.47	4.56
50	1.25	7.21	1.97
240 °C			
0	2.41	11.80	2.63
50	2.18	23.71	1.23

Table 13 Summary table of Bohart-Adams and Modified Dose-Response parameters of raw and pre-treated pine sawdust for Cr (VI) removal (pre-treatment conditions: 50% diethylene glycol, 50% H_2O, 0.045 N H_2SO_4, reaction time 50 minutes).

	Untreated	160 °C, 50 min	180 °C, 50 min	200 °C, 50 min	220 °C, 50 min
Bohart-Adams model					
n (mg·L^{-1})	101	1.217	2.092	1.708	521
K_L (L·mg^{-1}·min^{-1})	0.00043	0.00031	0.00025	0.00031	0.00014
SEE	6.509	5.012	31.282	4.404	4.202
Modified Dose-Response model					
q_o (mg g^{-1})	0.470	4.680	35.653	7.751	1.852
a_{mdr}	0.551	0.915	2.357	0.952	0.385
SEE	6.159	2.096	1.292	1.962	2.132

time of 50 minutes the value of n decreases and is equal to 521. In addition we observe that the q_o for the raw material is 0.47 mg·g^{-1} while for the raw material with 50% diethylene glycol, 50% H_2O, 0.045 N H_2SO_4, at 180 °C and an isothermal reaction time of 50 minutes equals 35.65 mg·g^{-1}, while again in the extreme pretreatment it decreases with a value of 1.85 mg·g^{-1}.

The Modified Dose-Response model shows that the raw material with 50% diethylene glycol, 50% H_2O, 0.045 N H_2SO_4, at 180 °C and an isothermal reaction time of 50 minutes increases its adsorption capacity by 75 times compared to the raw material, while in the

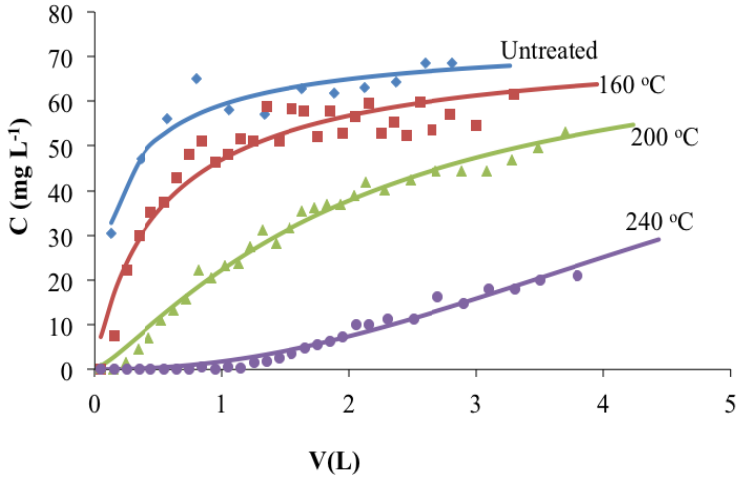

Fig. 12 Curves of Cr (VI) for C (mg·L^{-1}) as a function of V (mL) according to the Modified Dose-Response model for crude and self-hydrolyzed at 160, 200 and 240 °C for 50 minutes pine sawdust (adsorption conditions: x = 15 cm, E = 4.9 cm^2, Q = 20 mL·min^{-1}, m = 20 g, C_i = 75 mg·L^{-1}, pH = 2).

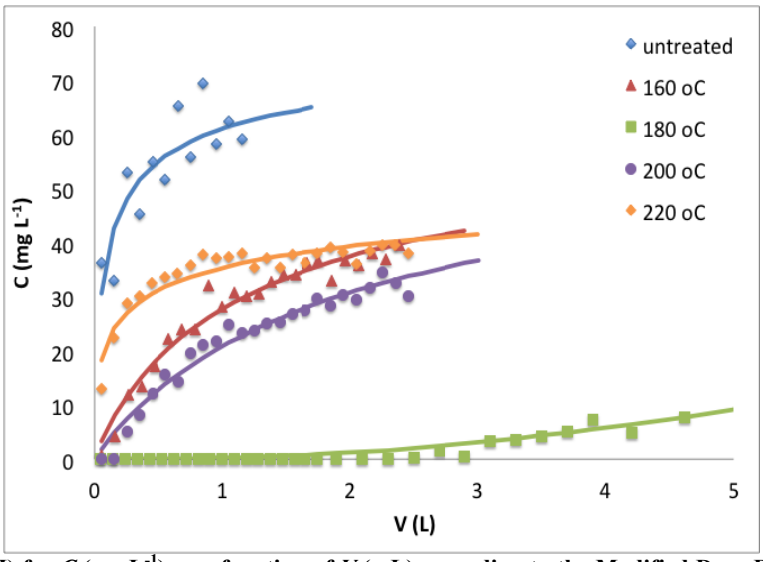

Fig. 13 Curves of Cr (VI) for C (mg·L^{-1}) as a function of V (mL) according to the Modified Dose-Response model for crude and pre-treated with 50% diethylene glycol, 50% H_2O, 0.045 N H_2SO_4, at 160-220 °C for 50 minutes pine sawdust (adsorption conditions: x = 15 cm, E = 4.9 cm^2, Q = 20 mL·min^{-1}, m = 20 g, C_i = 75 mg·L^{-1}, pH = 2).

raw material pre-treatment, i.e. at 220 °C for 50 minutes, the adsorption capacity of the material is higher than that of the raw material, but not the optimal one as we expected. The Fig. 12 shows the theoretical curves for the Modified Dose-Response model and for the four temperatures of the pre-treated spruce sawdust with an acid-catalyzed organic solvent. The adaptability of the Modified Dose-Response model to the experimental data was found to be better than that of the Bohart-Adams model for hexavalent chromium.

4. Conclusion

The experimental diagrams confirm the validity of the Freundlich equation for dilute solutions with low concentrations. At the same time, from the aggregate diagrams of the dilute solutions, listed above, we observe: For graph 1 concerning the adsorbent materials we used we observe that the capacity K_F has a higher value for the ground cork while the lower one for olive ash. Also, for graph 2, regarding the

adsorbent materials we used we observe the *n* of the isothermal Freundlich has a maximum for olive ash while a minimum has for two materials lentil straw and ground cork.

References

[1] Abo-Elela, S. I., and El-Dib, M. A. 1987. "Color Removal via Adsorption on Wood Shaving." *Sci. Tot. Envir.* 66: 269-73.

[2] Allen, S. J., Gan, Q., Matthews, R., and Johnson, P. A. 2003. "Comparison of Optimised Isotherm Models for Basic Dye Adsorption by Kudzu." *Biores. Techn.* 88: 143-52.

[3] Annadurai, G., Juang, R. S., and Lee, D. J. 2002. "Use of Cellulose Based Wastes for Adsorption of Dyes from Aqueous Solutions." *J. Hazard. Mater.* B92: 263-74.

[4] Bohart, G. S., and Adams, E. Q. 1920. "Adsorption in Columns." *J. Chem. Soc.* 42.

[5] Carrillo, F., Lis, M. J., and Valldeperas, J. 2002. "Sorption Isotherms and Behaviour of Direct Dyes on Lyocel Fibres." *Dyes & Pigments* 53: 129-36.

[6] Chubar, A., Carvalho, J. R., and Correia, M. J. N. 2004. "Heavy Metals Biosorption on Cork Biomass: Effect of the Pre-treatment." *Colloids and Surfaces A: Physicochem. Eng. Aspects.* 238: 51-8.

[7] Chun, L., Hongzhang, C., and Zuohu, L. 2003. "Adsorption of Cr(VI) by Fe-modified Steam Exploded Wheat Straw." *Proc. Biochem.*, in Press.

[8] Clark, R. M. 1987. "Modeling TOC Removal by GAC: The General Logistic Function." *J. Am. Wat. Works Assoc.* 79 (1): 33-7.

[9] Crank, G. 1993. *The Mathematics of Diffusion*. London, New York: Clarendon Press.

[10] El-Shobaky, G. A., and Youssef, A. M. 1978. "Chemical Activation of Charcoals." *Surface Techn.* 7 (3): 209-16.

[11] Garg, V. K., Gupta, R., Yadav, A. B., and Kumar, R. 2003. "Dye Removal from Aqueous Solutions by Adsorption on Treated Sawdust." *Biores. Techn.* 89: 121-4.

[12] Hutchins, R. A. 1973. "New Method Simplifies Design of Activated-Carbon Systems." *Chem. Eng.* 80 (19): 133.

[13] Ibrahim, N. A., Hashem, A., and Abou-Shosha, M. H. 1997. "Amination of Wood Sawdust for Removing Anionic Dyes from Aqueous Solutions." *Polym. Plast. Techol. & Eng.* 36 (6): 963-71.

[14] Jawaid, M. N. A., and Weber T. W. 1979. "Effect of Mineral Salts on Adsorption and Regeneration of Activated Carbon." *Carbon* 17 (2): 97-101.

Appendix: Determination of solution concentration with the help of a spectophotometer

Fig. 1A The spectrophotometer.

If I_0 and I_1 are the intensities of the incident in a solution and the radiation emitted from it, respectively, then the ratio I_0/I_1 is given by the relation: $-\log\frac{I_1}{I_0} = \varepsilon * c * l$

(Law Beer-Lambert)

where the left term of equality is called absorption A (formerly optical density),

ε = molecular absorption coefficient (formerly extinction coefficient), depending on the frequency of incident radiation (1/M * cm);

c = concentration of solution (M);

l = length of path followed by the radiation in the solution (cm).

The spectrophotometer is an instrument that measures the permeability $T = I_1/I_0$ and gives it as a fraction or percentage in the range

0-1 or 0-100%, respectively. At a special reading scale it gives the absorption directly $A = -\log\frac{I_1}{I_o}$.

If we measure the absorption of n solutions of different (known) concentration C_i (i = 1, 2, 3,…, n) in solute then it is possible to plot the pairs C_i, A_i as points on millimeter paper and draw the nearest straight line passing through them and from the beginning of the axes, after the expression

$$A = b * C, \quad b = \varepsilon * l \tag{1A}$$

is a simple analog relation without a fixed term. It goes without saying that, in order to use this relation, cells of equal thickness must be used so that the path of the radiation remains constant. For greater accuracy, the line is not drawn freely by hand, but the slope b is calculated with the help of the following ratio, which is extracted by linear regression by the least squares method (see annex):

$$b = \frac{\sum_{i=1}^{n} C_i A_i}{\sum_{i=1}^{n} C_i^{\,2}} \tag{2A}$$

A solution of unknown concentration C_x of the same dissolved is then given substance, the absorption of which is measured Ah. With the help of Eq. (1A) the value of the unknown concentration C_χ is calculated, since the value of parameter b has been previously estimated from Eq. (2A).

When the area in which C_x takes values is known, then we measure the absorption Ai of solutions of concentration C_i, i = 1, 2, 3, …, n that cover this area and we display these measurements on millimeter paper or with the help of H/PC as scatter diagrams. If the measurements seem to follow a non-linear course, then the unknown concentration C_x is determined by measuring the absorption A_x and Lagrange interference, which is achieved with the corresponding PC program. If the measurements appear to follow a linear course, then the linear model with a fixed term is used $A = a + bC,$ whose values of parameters a, b are estimated by linear regression by the method of least squares:

$$a = \frac{(\sum A_i)\left(\sum C_i^{\,2}\right) - \left(\sum C_i\right)\left(\sum C_i A_i\right)}{n\sum C_i^{\,2} - \left(\sum C_i\right)^2}$$

$$b = \frac{n\sum C_i A_i - \left(\sum C_i\right)\left(\sum A_i\right)}{n\sum C_i^{\,2} - \left(\sum C_i\right)^2}$$

After estimating the values of α, b, put them in the relation $A = \alpha + bC$ and calculate the unknown concentration C_χ of the solution whose absorbance A_χ is measured. The estimation of the SC_x error, performed with this calculation, is extremely complex, because we measure the dependent variable and calculate the independent one, i.e. we follow a reverse course of that indicated by the standard statistical analysis. In this case, most analysts use the relationship: $S_{C_\chi} = \frac{S_{A/C}}{b}\left[\frac{1}{m} + \frac{1}{n} + \frac{\left(A_\chi - \overline{A}\right)^2}{b^2\sum\left(C_i - \overline{C}\right)^2}\right]^{1/2}$

where n is the number of absorption measurements or solutions of a different known concentration (one measurement for each

solution). $\bar{A}$ is the average value of n absorption measurements. m is the number of measurements n samples of the same unknown solution (one measurement for each sample). Ah is the average value of m absorption measurements. SA/C is the error of estimating the dependent variable on the independent one, which is given by the expression:

$$S_{A/C} = \left[\frac{\sum (A_i - \hat{A}_i)^2}{n-2} \right]^{1/2}$$

$$\hat{A}_i = \alpha + bC_i,\ i = 1, 2, \ldots, n$$

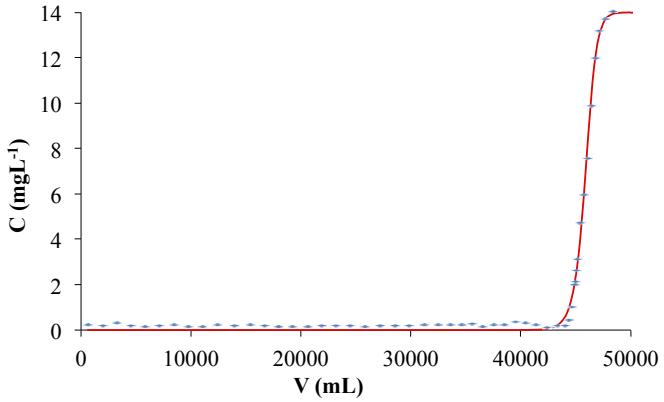

Fig. 2A Curves of methylene blue for C (mg·L^{-1}) as a function of V (mL) according to the Bohart-Adams model for raw pine sawdust (adsorption conditions: x = 15 cm, E = 4.9 cm^2, Q = 10 mL·min^{-1}, m = 22 g, C_i = 14 mg·L^{-1}, pH = 8).

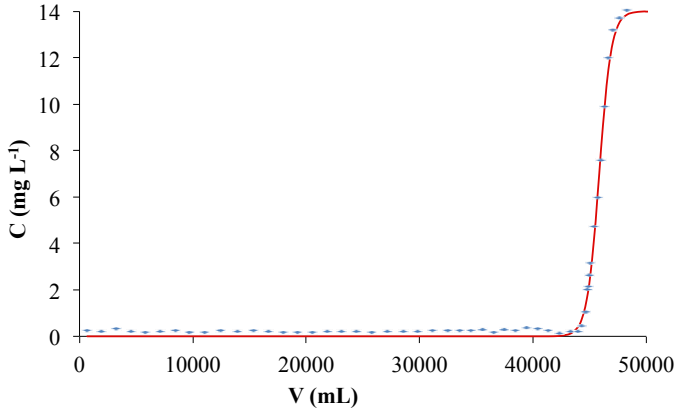

Fig. 3A Curves of methylene blue for C (mg·L^{-1}) as a function of V (mL) according to

Figs. 2A and 3A show the theoretical curves of MB for raw pine sawdust. The experiments were performed with a flow of 10 mL·min^{-1}, the mass of the material was 22 g and the concentration of MB dye was equal to 14 mg·L^{-1}. Fig. 2A shows the Bohart-Adams model and Figs. 3A shows the Clark model. According to the calculations of the Bohart-Adams model we have n = 8,722 mg·L^{-1}, K = 0.00134 L·mg^{-1}·min^{-1} and SEE = 0.194 while according to the Clark model we have n = 8,781 mg·L^{-1}, K = 0 , 00159 L·mg^{-1}·min^{-1} and SEE = 0.201. Observing the above we can say that the Bohart-Adams model adapts better to our experimental data than the Clark model for the methylene blue dye.

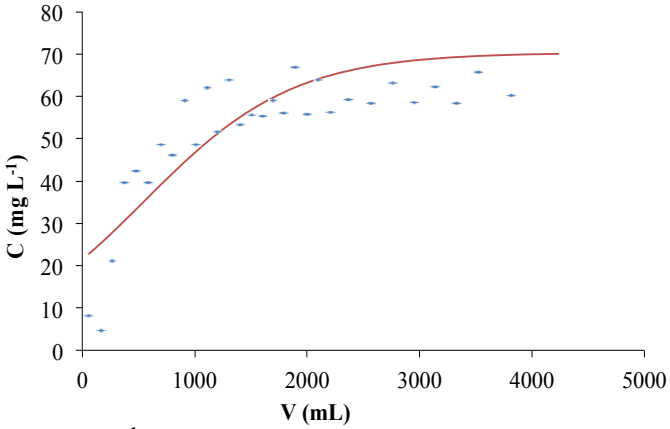

Fig. 4A Curves of Cr (VI) for C (mg·L^{-1}) as a function of V (mL) according to the Bohart-Adams model for raw pine sawdust (adsorption conditions: x = 15 cm, E = 4.9 cm^2, Q = 10 mL·min^{-1}, m = 24 g, C_i = 70 mg·L^{-1}, pH = 2).

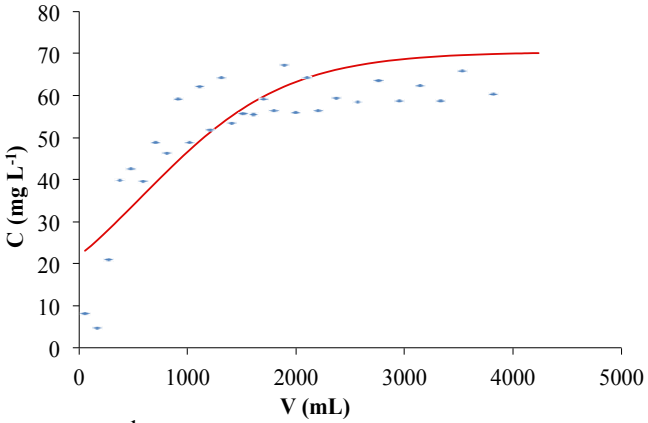

Fig. 5A Curves of Cr (VI) for C (mg·L^{-1}) as a function of V (mL) according to the Clark model for raw pine sawdust (adsorption conditions: x = 15 cm, E = 4.9 cm^2, Q = 10 mL·min^{-1}, m = 24 g, C_i = 70 mg·L^{-1}, pH = 2).

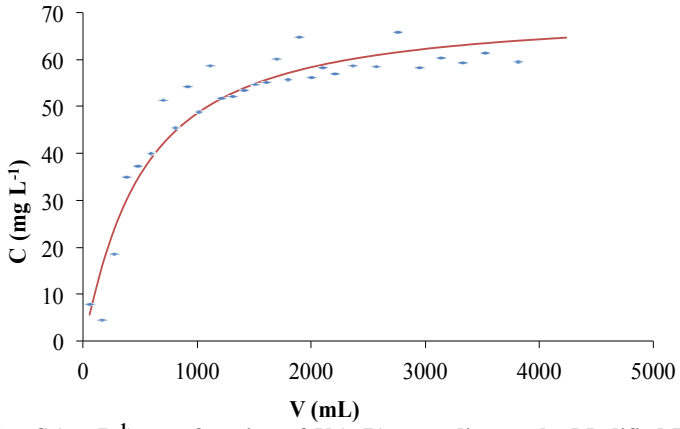

Fig. 6A Curves of Cr (VI) for C (mg·L^{-1}) as a function of V (mL) according to the Modified Dose-Response model for raw pine sawdust (adsorption conditions: x = 15 cm, E = 4.9 cm^2, Q = 10 mL·min^{-1}, m = 24 g, C_i = 70 mg·L^{-1}, pH = 2).

Figs. 4A-6A show the theoretical curves of Cr (VI) for raw pine sawdust. The experiments were performed at a flow rate of 10 mL·min^{-1}, the mass of the material was 24 g and the concentration of hexavalent chromium was 70 mg·L^{-1}. According to the calculations of the Bohart-Adams model we have n = 524 mg·L^{-1}, K = 0.00022 L·mg^{-1}·min^{-1} and SEE = 9.03, according to the Clark model we have n = 615 mg·L^{-1}, K = 0.00023 L·mg^{-1}·min^{-1} and SEE = 9.09 while for the Modified Dose-Response model we have a_{mdr}

= 1.1334, b_{mdr} = 0.494, q_0 = 2.897 mg·g^{-1}, *SEE* = 4.57. Observing the above we can say that the Modified Dose-Response model adapts better to our experimental data than the other two models for hexavalent chromium.

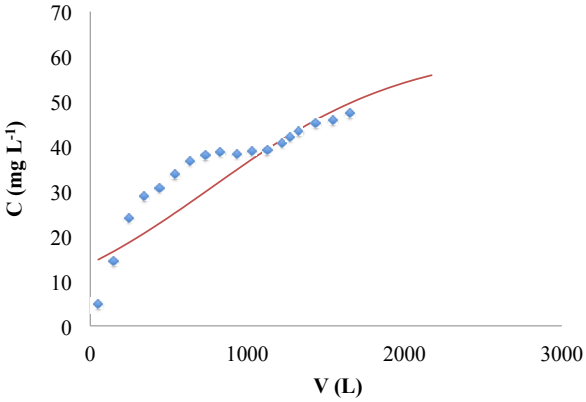

Fig. 7A Curves of Cr (VI) for *C* (mg·L^{-1}) as a function of *V* (mL) according to Bohart-Adams model for crude spruce sawdust (adsorption conditions: *x* = 15 cm, *E* = 4.9 cm^2, *Q* = 10 mL·min^{-1}, *m* = 20 g, C_i = 70 mg·L^{-1}, *pH* = 2).

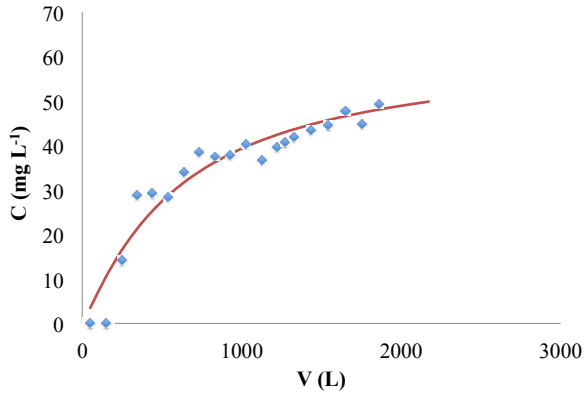

Fig. 8A Curves of Cr (VI) for *C* (mg·L^{-1}) as a function of *V* (mL) according to the Modified Dose Response model for crude spruce sawdust (adsorption conditions: *x* = 15 cm, *E* = 4.9 cm^2, *Q* = 10 mL·min^{-1}, *m* = 20 g, C_i = 70 mg·L^{-1}, *pH* = 2).

Figs. 7A and 8A. above show the theoretical curves of Cr (VI) for crude spruce sawdust. The experiments were performed at a flow rate of 10 mL·min^{-1}, the mass of the material was 20 g and the concentration of hexavalent chromium was 70 mg·L^{-1}. According to the calculations of the Bohart-Adams model we have *n* = 651 mg·L^{-1}, *K* = 0.00031 L·mg^{-1}·min^{-1} and *SEE* = 7.01 while for the Modified Dose-Response model we have a_{mdr} = 1.125, b_{mdr} = 0.608, q_0 = 3.760 mg·g^{-1}, *SEE* = 3.89. Observing the above we can say that the Modified Dose-Response model adapts better to our experimental data for hexavalent chromium.